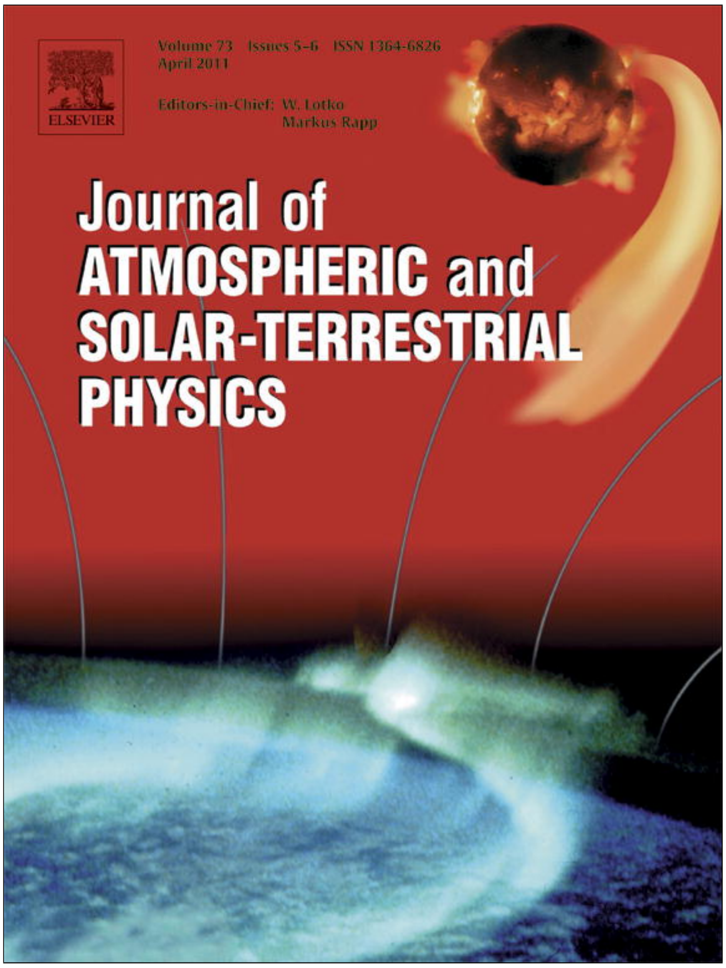
Volume 73 Issues 5–6 ISSN 1364-6826
April 2011
Editors-in-Chief: W. Lotko
Markus Rapp
ELSEVIER
Journal of
ATMOSPHERIC and
SOLAR-TERRESTRIAL
PHYSICS

Journal of Atmospheric and Solar-Terrestrial Physics 73 (2011) 664–670

Contents lists available at ScienceDirect

Journal of Atmospheric and Solar-Terrestrial Physics

journal homepage: www.elsevier.com/locate/jastp

Generation of VHF radio emissions by electric discharges in the lower atmosphere over a seismic region

V.M. Sorokin [a,*], Yu.Ya. Ruzhin [a], A.K. Yaschenko [a], M. Hayakawa [b]

[a] Puskov Institute of Terrestrial Magnetism, Ionosphere and Radio Wave Propagation (IZMIRAN), Russian Academy of Sciences, Troitsk, Moscow Region 142190, Russian Federation
[b] The University of Electro-Communications, Department of Electronic Engineering, Chofu Tokyo, Japan

ARTICLE INFO

Article history:
Received 30 June 2010
Received in revised form
4 December 2010
Accepted 17 January 2011
Available online 1 February 2011

Keywords:
VHF radio emission
Electric discharges
Earthquake precursors

ABSTRACT

Observational data of the seismic related VHF radio emissions at 41 and 53 MHz obtained at the four stations of Create Island are presented. The epicenter of EQs is located at the distance more than 300 km behind the horizon. It was shown that VHF radiation is generated at the altitudes 1–10 km in the atmosphere over the epicenter of EQs. The theory of generation of electromagnetic radiation by random electric discharges was developed. These discharges are excited by DC electric field enhanced up to the breakdown value in the atmosphere. The field is connected with the electric current flowing in the atmosphere–ionosphere circuit, whose source is generated by convective transport of charged aerosols, which are injected in the atmosphere by soil gases during the enhancement of seismicity. Calculations of the spectrum of electromagnetic radiation are derived, and the theoretical results are confirmed by observation data.

1. Introduction

Recently it is well known that a lot of electromagnetic effects in different frequency ranges which are related to seismicity are observed (Hayakawa and Molchanov, 2002; Molchanov and Hayakawa, 2008; Hayakawa, 2009). We think that the VHF radiation related to EQ preparation is the least investigated. Let us present several observational results of the VHF anomaly phenomena. Based on the radio-locator data, Voinov et al. (1992) revealed the appearance of distributed electric charges above the epicenter 1–3 days before the Spitak EQ. The area of charges distribution was different from those occurred during thunderstorms. The lifetime of such a seismogenic charged area was several hours, while the lifetime of the same area during thunderstorms does not exceed one hour (Proctor, 1981). The altitude and scattering cross section of those areas of seismogenic charges had some unusual values. The altitude was 5–30 km and the scattering cross section exceeded by 10 times the same one for the thunderstorm (Warwick et al., 1979). Voinov et al. (1992) suggested that distributed electric charges could be the source of discharges, which formed an anomaly during the radio-astronomy observation at the frequency of 75 MHz. Hata et al. (1998) revealed 225 Hz electromagnetic radiations generated close to the sea surface during seismicity and volcanic activity in the zone of underwater faults. Localization of the radiation source had been performed by measuring the magnetic components of radiation (Hata et al., 1996). The glow of sky at distance of 100–200 km from the epicenter on the eve of a powerful EQ ($M = 7.3$) in China was observed at night (Zhao and Qian, 1997). Williams (1989) then noted that the seismic related airglow can reach altitudes more than 1–2 km at distance 140 km from the epicenter.

For the first time, the regular observation of pre-EQ anomalies in VHF electromagnetic radiation had been carried out on Create Island for three years starting from 1992. This observation was carried out using receivers with two frequencies 41 and 53 MHz located on the four sites (Nomicos et al., 1995; Vallianatos and Nomicos, 1998), and the pre-EQ VHF radiation had been registered. The center of EQs was located both on the ground and under the sea bottom. Based on the obtained data Ruzhin et al. (1999, 2000) have shown that the possible VHF radiation source is located in the atmosphere at altitudes of several km above the epicenter of preparing EQs. It was suggested that the generation of VHF radiation could be occurred as a result of electric discharges connected with convective transport of the charged aerosols at altitudes of 1–10 km in the zone of EQ preparation.

Later, Yamada et al. (2002) confirmed this conclusion that VHF radiation sources are located in the atmosphere at altitudes over several kilometers. VHF radiation (52.1–52.5 MHz) related to an EQ was obtained as a result of long-term observations from July 1999. Direction to the EQ epicenters was in the limits of antenna diagram. The distance to epicenters was several hundreds of kilometers, and therefore it was possible to register radiation if

* Corresponding author. Tel.: +7 495 330 9902; fax: +7 496 751 0124.
E-mail address: sova@izmiran.ru (V.M. Sorokin).

1364-6826/$ - see front matter
doi:10.1016/j.jastp.2011.01.016

its source was located in the atmosphere at altitude of several kilometers.

Yonaiguchi et al. (2007) investigated the fractal character of VHF radiation on frequency 49.5 MHz, which occurred on the eve of an EQ ($M=7.2$) on August 16, 2005. The observations were made on three stations in the nearby zone located at the distances in dozens of kilometers from the epicenter. It was assumed that the occurrence of such radiation depends on geological characteristics of the ground surface.

Further, Hayakawa et al. (2006) have found the strong VHF radio noise (77.1 MHz) as a precursor to the 2004 Mid Niigata prefecture EQ (October 23). On October 15–18 they have detected the VHF radio noises, and their direction finding has indicated that those noises are coming close to the direction of the EQ epicenter. Yasuda et al. (2009) have developed an interferometic VHF system and have found that the VHF radio noises are always simultaneously detected with the over-horizon VHF transmitter signal (77.1 MHz), with their azimuths being relatively close to the epicenter of the EQ.

2. The results of observation of VHF electromagnetic radiation related to seismicity

As it was mentioned above, VHF electromagnetic EQ precursors were registered by a network of four stations of Create Island (Nomicos et al., 1995; Vallianatos and Nomicos, 1998). Since 1992 the special network of telemetric stations were created on this island for investigation of the electromagnetic precursors. On each station the VHF radio noise on frequency 41 and 53 MHz, is measured as one of different parameters. These radiations are found to have occurred for several days before an EQ, and their duration reaches several days. If VHF electromagnetic radiation is propagated over the distance more than a wavelength $\lambda \approx 6\text{-}7.5$ m, the condition of optical propagation is fulfilled. Consequently, it is possible to receive the signal at distance of the order of 300 km just in the case if its source is located in the atmosphere above Earth's surface. According to Ruzhin and Nomicos (2007) the region of generation of VHF electromagnetic radiation is at the altitudes of the order of several kilometers above EQ epicenters located behind the horizon. An example of anomalous signals recorded on the frequency of 41 and 53 MHz on the eve of an EQ on November 21, 1992 is presented in Fig. 1. The records have been obtained on all the stations of the network along Create Island (Nipos, Ierapetra, Heraklio and Drapania). One can see that signals at both frequencies are registered on the stations 3 and 4. The signal at the frequency of 41 MHz is the same one at the frequency 53 MHz. The absence of the signal at the station Ierapetra (I) can be explained in term of both the radio shadow by mountains and the small altitude of radiation source. Namely, its altitude must be smaller, such as 2950 m above the sea level near the epicenter.

The frequencies 41 and 53 MHz of radio waves had been chosen for electromagnetic monitoring on Create Island because the signal-to-noise ratio is an optimal one for this frequency range. Radio-astronomical observation and lightning discharges registration are usually carried out in this frequency range. It is known that the spectrum of electromagnetic radiation of thunderstorm discharges decreases with frequency, while the typical spectrum of natural noise falls down more sharply already in the beginning of frequency range 3–30 MHz. Such a character of the spectrum corresponds to the maximum of signal-to-noise ratio in the frequency range 20–100 MHz (Taylor, 1978). Noise analyses which were derived by Ruzhin and Nomicos (2007) allow us to conclude that observed signals were generated by the seismic origin. Let us specify the general results obtained by the observation of VHF electromagnetic radiation. Their differences from earlier obtained data (Warwick et al., 1982; Maeda and Tokimasa, 1996) are as follows:

- VHF signal was registered for a lot of EQs from the continuous observations during three years.
- VHF signal was registered on two frequencies 41 and 53 MHz repeatedly and on several stations simultaneously.
- Sources of pre-seismic VHF radiation were located behind the radio horizon at distances 300–350 km from the receivers.
- Signal was observed for several days before EQs both at day and at night.
- Center of sea EQs was located under the sea bottom, while the source of radiation was located in the atmosphere above the sea surface.

3. Discharges region in the lower atmosphere

Let us assume that the electric discharges are the source of electromagnetic radiation. These discharges take place in the region of atmosphere, in which electric field reaches the breakdown value, and the source of field has to be in operation for several days. During this time there is an observed significant growth of DC electric field over a seismic region in such a way that the magnitude of field reaches up to 10 mV/m in the ionosphere (Chmyrev et al., 1989; Gousheva et al., 2008). According to electrodynamic model of the atmosphere–ionosphere coupling, such a field enhancement is related to the generation of electric

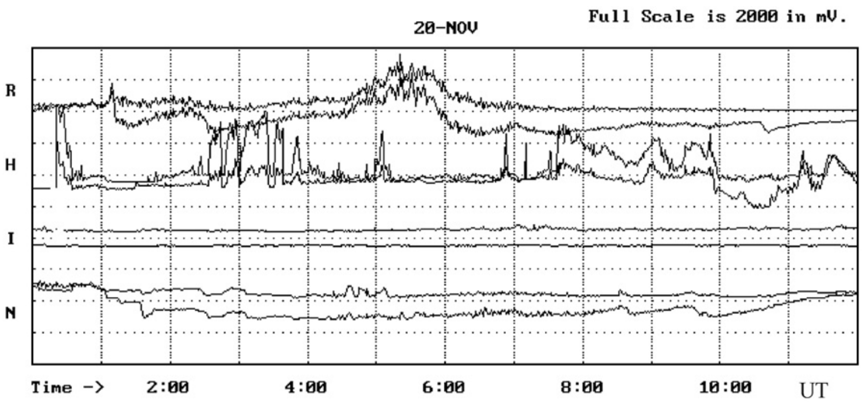

Fig. 1. The pre-seismic VHF signals for the November 21, 1992 EQ ($M=6.0$). The output voltage of the receivers presented is given on the vertical axis. Full scale is 2000 mV (Ruzhin and Nomicos, 2007). N, I, H and D represent the observing stations of Nipos, Ierapetra, Heraklio and Drapania, respectively, forming Crete monitoring station.

current in the atmosphere–ionosphere circuit (Sorokin et al., 2001, 2007; Sorokin and Chmyrev, 2002, 2010). The source of current is an electromotive force (EMF) occurring by charged aerosols injected in the atmosphere during EQ preparation. Below we use this model in the interpretation of generation of VHF radio emissions in the atmosphere over an EQ zone.

We consider the altitude distribution of electric field in the atmosphere over a seismic region. The electric field of conducting current is generated by EMF in the near-Earth atmosphere. An external current of EMF arises as a result of emanation of charged aerosols transported into the atmosphere by soil gases and subsequent processes of upward transfer, gravitational sedimentation and charge relaxation. The field limitation on the Earth surface is caused by a feedback mechanism between excited electric field and the causal external current. This feedback is produced by the potential barrier for charged particles at their transfer from ground to the atmosphere. Atmospheric radioactivity produces influence to the external current and conductivity of the lower atmosphere.

Let us consider generation of the electric field by the external current $\mathbf{j}_e$ in the Earth-ionosphere layer (Sorokin et al., 2005, 2006). We will derive the equations for potential φ of the electric field disturbance $\mathbf{E}=-\nabla\cdot\varphi$. We introduce the Cartesian coordinates (x, y, z) with the axis z being directed vertically upward, and the homogeneous magnetic field $\mathbf{B}$ is directed with angle α to the x axis. The plane $y=0$ coincides with the absolutely conductive Earth's surface, and we assume that the electric field potential on this surface is $\varphi|_{z=0}=0$. The atmosphere characterized by the conductivity $\sigma(z)$ is located in the layer $0<z<z_1$. The plane $z=z_1$ coincides with the thin conducting ionosphere characterized by the tensor of integral conductivity with components Σ_P, Σ_H (Pedersen and Hall conductivities, respectively). For the slow processes with characteristic durations $t \gg \varepsilon_0/\sigma$ the electric potential φ in the atmosphere is derived from the equation of continuity and Ohm's law

$$\nabla\cdot(\sigma\,\nabla\cdot\varphi-\mathbf{j}_e)=0.$$

Injection of the charged aerosols in the atmosphere results in the appearance of potential barrier on the Earth surface, which leads to the limitation of electric field. Sorokin et al. (2006) found the electric field generated by the external current in the atmosphere whose vertical component is given in the form

$$j_e(r,z)=j_p(r)s_p(z)-j_n(r)s_n(z);$$
$$r=\sqrt{x^2+y^2}.$$

where j_p and j_n are the density of external currents, which are formed by positive and negative charged aerosols, respectively, and j_e is the density of total external current. The vertical component of electric field $E_z(r,z)$in the atmosphere–ionosphere layer is derived from the equation (Sorokin et al., 2006, 2007)

$$E_z(r,z)=\frac{1}{\sigma(z)}\left[\left(\frac{k_p}{\rho}-s_p(z)\right)j_p(r)\sqrt{1+\frac{E_z(r,0)}{E_c}}-\left(\frac{k_n}{\rho}-s_n(z)\right)\times j_n(r)\sqrt{1-\frac{E_z(r,0)}{E_c}}\right]. \quad (1)$$

The equations for calculating the electric field potential $\varphi_1(x, y)$ and the horizontal components of electric field in the ionosphere have a form

$$\left(\frac{1}{\sin^2\alpha}\frac{\partial^2}{\partial x^2}+\frac{\partial^2}{\partial y^2}\right)\varphi_1(x,y)=-\frac{1}{2\rho\Sigma_P}\left[k_pj_p(r)\sqrt{1+\frac{E_z(r,0)}{E_c}}-k_nj_n(r)\sqrt{1-\frac{E_z(r,0)}{E_c}}\right]E_x(x,y)=-\partial\varphi_1(x,y)/\partial x;\quad E_y(x,y)=-\partial\varphi_1(x,y)/\partial y. \quad (2)$$

In Eqs. (1) and (2) we identify

$$k_p=\int_0^{z_1}dz\frac{s_p(z)}{\sigma(z)};\quad k_n=\int_0^{z_1}dz\frac{s_n(z)}{\sigma(z)};\quad \rho=\int_0^{z_1}\frac{dz}{\sigma(z)}.$$

The critical field E_c can be estimated from the balance between viscosity, gravity and electrostatic forces. The estimation of critical field $E_c=450\,V/m$ was performed in Sorokin et al. (2005). Sorokin et al. (2006, 2007) made computations of DC electric field both in the ionosphere and in the atmosphere, and below we will use these results for creation of the origin of VHF emissions.

Let us choose the axial symmetric distribution of external current in the lower atmosphere in the form

$$j_e(r,z)=[j_{p0}s_p(z)-j_{n0}s_n(z)]\exp(-r^2/r_0^2).$$

where $s_{p,n}(z)$ and $\sigma(z)$ are the altitude dependences of external current and conductivity, respectively, j_{p0}, j_{n0} are the density of external currents, which are formed by positive and negative charged aerosols in the epicenter, respectively, and r_0 is the horizontal scale of external current. Sorokin et al. (2006) also calculated the horizontal distribution of electric field in the ionosphere, and the result of calculation is depicted in Fig. 2. Estimation of the critical field gives a value E_c=450 V/m. This graph shows that DC electric field reaches up to 10 mV/m in the

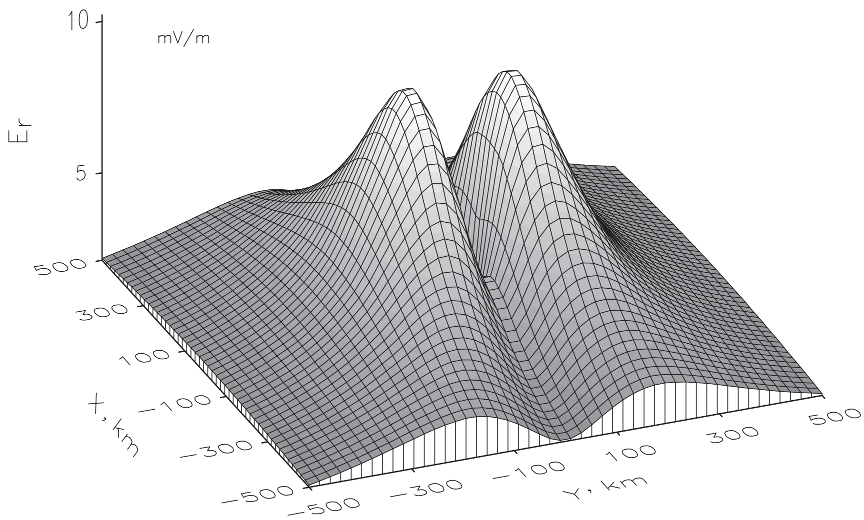

Fig. 2. Calculation results of the spatial distribution of radial component of electric field in the ionosphere (Sorokin et al., 2006).

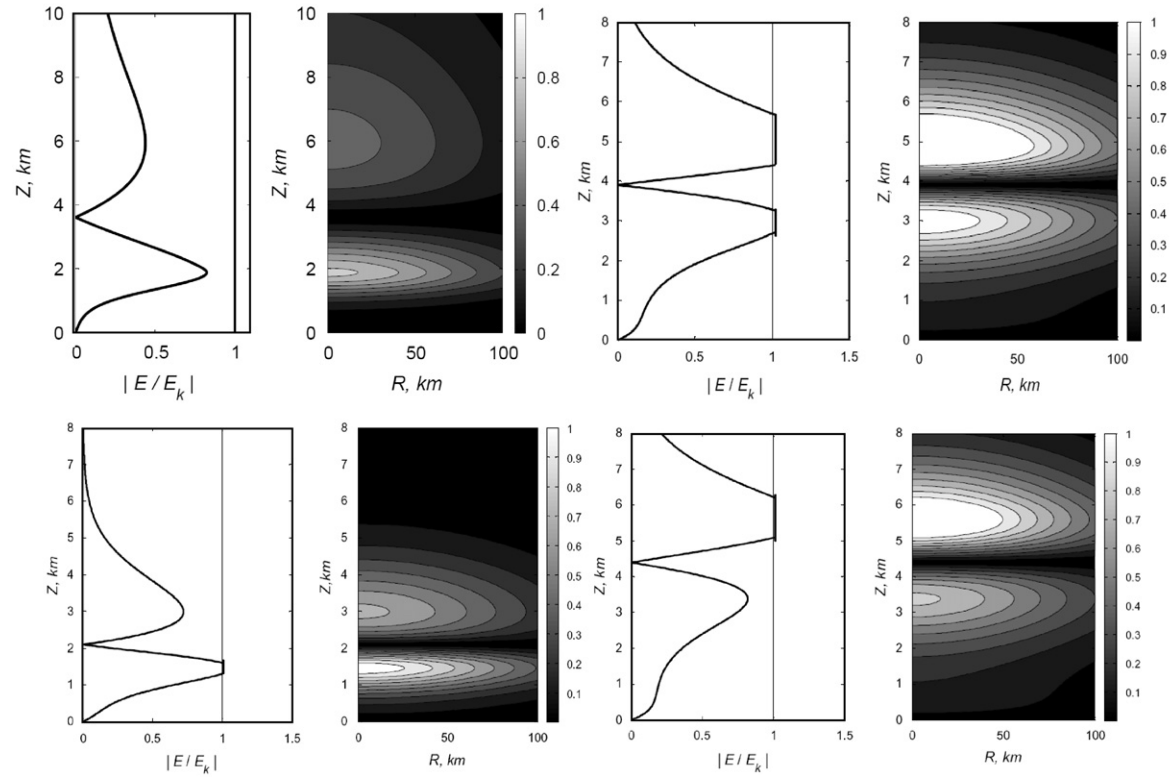

Fig. 3. Altitude distribution of the electric field amplitude relative to its breakdown value. The following parameters are chosen for calculations $r_0 = 100\,\text{km}$, $j_{n0}/j_{p0} = 0.6$: left graphics: $r_p = 5\times10^{-6}\,\text{m}$, $r_n = 7\times10^{-6}\,\text{m}$, $h_u = 2\times10^{3}\,\text{m}$, $u_0 = 2.3\times10^{-2}\,m/s$; upper panel: $j_{p0} = 1.4\times10^{-9}\,A/m^2$; lower panel: $j_{p0} = 1.3\times10^{-9}\,A/m^2$; right graphics: $r_p = 10\times10^{-6}\,\text{m}$, $r_n = 12\times10^{-6}\,\text{m}$, $u_0 = 3.2\times10^{-2}\,m/s$, $j_{p0} = 1.3\times10^{-9}\,A/m^2$; upper panel: $h_u = 5\times10^{3}\,\text{m}$; lower panel: $h_u = 6\times10^{3}\,\text{m}$.

ionosphere. The calculation results are confirmed by numerous satellite data on direct measurements of enhancement of DC electric field in the ionosphere. For example, Chmyrev et al. (1989) and Gousheva et al. (2008) found that DC electric field reaches up to 10 mV/m and even more in the ionosphere during several days before EQs. Experimental confirmation of the calculation results by Eqs. (1) and (2) of DC electric field in the ionosphere allows us to use Eq. (1) to determine the altitude distribution of electric field in the atmosphere. The method for computing the electric field in the atmosphere was developed in Sorokin et al. (2007), from which we use functions $s_{p,n}(z)$ and $\sigma(z)$. The external current is formed by vertical transfer of positive and negative charged aerosols, which have radii r_p and r_n respectively. The aerosols are moved by atmosphere convection with velocity u^0 in the layer of atmosphere with vertical scale h_u. Based on Sorokin et al. (2007) we have calculated the altitude distribution of electric field for different value of these parameters. Corresponding calculation results are presented in Fig. 3, where E_k is the breakdown field. The graphs show that the growth of aerosols radius and intensification of atmosphere convection leads to an increase in electric field. It is possible to expect the electric discharges in one or two regions located at different altitudes in which the electric field reaches a breakdown value.

4. Generation of VHF radio emissions in the atmosphere

DC electric field is shown above which can be reached to the breakdown value, and electric discharges are known to occur in this region. Let us suggest that the discharge is excited substantially by a vertical component of electric field and it is an electric dipole. We consider an electromagnetic radiation of the impulse

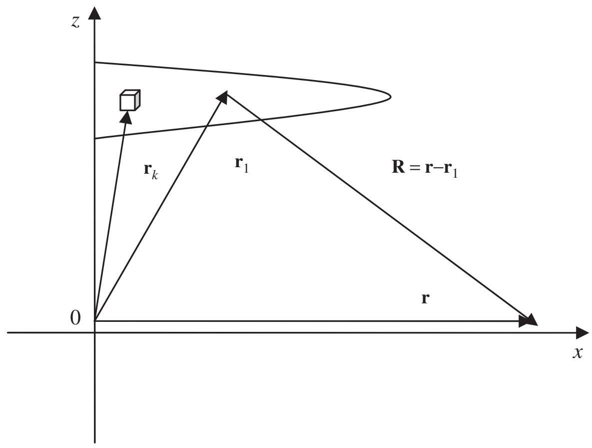

Fig. 4. Coordinates used for the calculation of characteristics of electromagnetic radiation.

electric dipoles. The electric field **E** and magnetic field **H** of their radiation are expressed by Maxwell equations

$$\nabla\times\mathbf{H} = \mathbf{j} + \varepsilon_0\frac{\partial\mathbf{E}}{\partial t};\quad \nabla\times\mathbf{E} = -\mu_0\frac{\partial\mathbf{H}}{\partial t}$$

$$\nabla\cdot\mathbf{E} = \frac{q}{\varepsilon_0};\quad \nabla\cdot\mathbf{H} = 0.$$

where **j** is the electric current density of electric current of dipoles, q is the density of their charges, ε_0 is the electric constant of free space and μ_0 is the permeability of vacuum. Let us denote the vertical components of electric field and current as $E_z \equiv E$; $j_z \equiv j$ in the Cartesian coordinates (x, y, z) presented in Fig. 4. We assume the discharge region of atmosphere to be as cells. Each center of the cell is located at the points with radius-vector $\mathbf{r}_k$ as depicted in Fig. 4. The current density $\mathbf{j}$ is formed as a result of random discharges. One assumes that the dependence of current density on the coordinate $\mathbf{r}$ and time t is defined by the function

$$\mathbf{j}(\mathbf{r},t)=\sum_{k,m}\mathbf{j}_k A(\mathbf{r}-\mathbf{r}_k,t-t_{km}). \tag{3}$$

where $\mathbf{j}_k$ is the current density of a random discharge in the cell with number k, t_{km} is the time of occurrence of the statistically independent discharges in the cell with number k and $A(\mathbf{r}-\mathbf{r}_k,t-t_{km})$is the dimensionless current density of electric discharge in the cell with radius-vector $\mathbf{r}_k$ which occurred at time t_{km}.

We suggest that all values are dependent on time as $\exp(-i\omega t)$. The electric field is defined by the equation in the wave zone ($kr \gg 1$) on the surface of perfectly conducting Earth

$$E(\mathbf{r},\omega)=\int_V j(\mathbf{r}_1,\omega)G(\mathbf{r}-\mathbf{r}_1,\omega)\,d\mathbf{r}_1;$$
$$G(\mathbf{r}-\mathbf{r}_1,\omega)=\frac{i\omega\mu_0}{2\pi}\left(1-\frac{z_1^2}{R^2}\right)\frac{\exp(ikR)}{R};\quad R=|\mathbf{r}-\mathbf{r}_1|. \tag{4}$$

where the vector $\mathbf{r}_1$ has the components (x_1, y_1, z_1). Using Fourier transform to Eq. (3), one finds

$$j(\mathbf{r},\omega)=\sum_{k,m} j_k\, A(\mathbf{r}-\mathbf{r}_k,\omega)\exp(i\omega t_{km}). \tag{5}$$

Phases ωt_{km} are the independent random values, which are distributed as Poisson flow (Rytov et al., 1978) in the interval $(0-2\pi)$

$$\langle \exp(i\omega t_{km})\rangle=0;\quad \langle \exp(i\omega t_{km})\exp(-i\omega t_{in})\rangle=\delta_{ki}\delta_{mn}. \tag{6}$$

where angle brackets denote a statistical averaging (Rytov et al., 1978). Substituting Eq. (5) in (4) we find

$$E(\mathbf{r},\omega)=\sum_k E_k(\mathbf{r},\omega)\sum_m \exp(i\omega t_{km})$$
$$E_k(\mathbf{r},\omega)=j_k\int_V A(\mathbf{r}'-\mathbf{r}_k,\omega)G(\mathbf{r}-\mathbf{r}',\omega)\,d\mathbf{r}'. \tag{7}$$

where $E_k(\mathbf{r},\omega)$ is the electric field radiated by the discharge in the cell with number k. In Eq. (7) the integration is carried out over the volume of discharges region. Substituting Eq. (7) in (6), one finds $\langle E(\mathbf{r},\omega)\rangle=0$. If the size of source is smaller than the wavelength of radiation Eq. (7) is transformed to the following equality:

$$E(\mathbf{r},\omega)\approx a(\omega)\sum_k j_k G(\mathbf{r}-\mathbf{r}_k,\omega)\sum_m \exp(i\omega t_{km})$$
$$a(\omega)=\int_V A(\mathbf{r}',\omega)\,d\mathbf{r}'. \tag{8}$$

Power spectrum $P(\mathbf{r},\omega)$ of the electromagnetic radiation of discharges, which is observed during an interval of time T, is defined by the formula

$$P(\mathbf{r},\omega)=\lim_{T\to\infty}\frac{|E_T(\mathbf{r},\omega)|^2}{T};\quad E_T(\mathbf{r},\omega)=\int_0^T \exp(i\omega t)E(\mathbf{r},t)\,dt.$$

The frequency spectrum of electric field of radiation $E(\mathbf{r},\omega)$ is defined by the power spectrum

$$E(\mathbf{r},\omega)=\sqrt{P(\mathbf{r},\omega)}. \tag{9}$$

Let us introduce the cylindrical coordinates (ρ, φ, z) with the origin of coordinates located in the epicenter of an EQ. The calculation of power spectrum has been derived in Appendix (formula (A4))

$$P(\rho,\omega)=\langle j_k^2\rangle|a(\omega)|^2\frac{\mu_0^2 v\omega^2}{2\pi}\int_0^\infty \rho_1 d\rho_1\int_0^\infty dz_1\frac{g(\rho_1,z_1)}{r^2\sqrt{1-p^2}}$$
$$\times\left[1-\frac{2z_1^2}{r^2}\frac{1}{1-p^2}+\frac{z_1^4}{r^4}\frac{1+p^2/2}{(1-p^2)^2}\right]. \tag{10}$$

Let us suggest that a discharge is an infinitely thin pulse linear current flowing on the line segment l. This current arises in the cell with number k at the moment of time t_{km}. Their spatial temporal distribution is chosen in the form

$$A(\mathbf{r}-\mathbf{r}_k,t-t_{km})=B(z-z_k,t-t_{km})s\delta(x-x_k)\delta(y-y_k). \tag{11}$$

where $\delta(x)$ is the Dirac delta function, and s is the square of cross-section of discharge. Substituting Eq. (11) in (8) yields

$$a(\omega)=s\int_{-l/2}^{l/2} B(z,\omega)\,dz. \tag{12}$$

We use the model of distribution of linear current in the discharge which has been presented in Iudin and Trakhtengerts (2001). Corresponding formula has the form

$$B(z,t)=\left\{\eta\left(t-\frac{z}{u}\right)\left[e^{-\alpha(t-z/u)}-e^{-\beta(t-z/u)}\right]-\eta(t-\tau)\right.$$
$$\left.\times[e^{-\alpha(t-\tau)}-e^{-\beta(t-\tau)}]\right\}\eta\left(\frac{l}{2}-|z|\right).$$

where u is the velocity of current wave in the discharge, $\tau=l/u$, $\eta(x)$ is the Heaviside unit function. According to the data from Berger et al. (1975) we choose the prameters in this formula in the form $\alpha=2/\tau$; $\beta=8/\tau$. Substituting this equation in Eq. (12), we obtain

$$\langle j_k^2\rangle|a(\omega)|^2=\frac{I_0^2(\beta-\alpha)^2u^2}{\omega^2(\alpha^2+\omega^2)(\beta^2+\omega^2)}|(1-i\omega\tau)\exp(i\omega\tau)-1|^2. \tag{13}$$

In Eq. (13) $I_0=\sqrt{\langle I_k^2\rangle}$ is the mean-square value of linear current amplitudes of discharges in the cells, and $I_k=sj_k$ is the amplitude of linear current of discharge in the cell with number k. Substituting Eq.(13) in (10) one finds the power spectrum of radiation in the form

$$P(\rho,\omega)=\mu_0^2I_0^2\frac{v}{2\pi}\frac{(\beta-\alpha)^2u^2}{(\alpha^2+\omega^2)(\beta^2+\omega^2)}|(1-i\omega\tau)\exp(i\omega\tau)-1|^2H^2(\rho)$$
$$H^2(\rho)=\int_0^\infty \rho_1 d\rho_1\int_0^\infty dz_1\frac{g(\rho_1,z_1)}{r^2\sqrt{1-p^2}}\left[1-\frac{2z_1^2}{r^2}\frac{1}{1-p^2}+\frac{z_1^4}{r^4}\frac{1+p^2/2}{(1-p^2)^2}\right]$$
$$r^2=\rho^2+\rho_1^2+z_1^2;\quad p=\frac{2\rho\rho_1}{r^2}. \tag{14}$$

Substituting Eq. (14) in (9) one finds the spectrum of electric field of radiation at a distance ρ from the epicenter of disturbed region of the atmosphere

$$E(\rho,\omega)=\mu_0I_0\sqrt{\frac{v}{2\pi}}\frac{u(\beta-\alpha)}{\sqrt{(\alpha^2+\omega^2)(\beta^2+\omega^2)}}|(1-i\omega\tau)\exp(i\omega\tau)-1|H(\rho);$$
$$H(\rho)=\sqrt{\int_0^\infty \rho_1 d\rho_1\int_0^\infty dz_1\frac{g(\rho_1,z_1)}{r^2\sqrt{1-p^2}}\left[1-\frac{2z_1^2}{r^2}\frac{1}{1-p^2}+\frac{z_1^4}{r^4}\frac{1+p^2/2}{(1-p^2)^2}\right]}. \tag{15}$$

According to Eqs. (14) and (15), the power spectrum of electromagnetic radiation and the spectrum of their electric field are defined by the spatial distribution of probability density of discharges $g(\rho, z)$ occurring in the atmosphere region, in which the electric field can reach the breakdown value. The probability density has the maximal value in the center of this region and it decreases depending on the epicentral distance. We choose such a spatial distribution of the probability density in the form

$$g(\rho,z)=\frac{3}{2\pi hd^2}\left(1-\frac{\rho^2}{d^2}\right)\left[1-\left(\frac{z-z_0}{h}\right)^2\right]\eta(d-\rho)\eta(h-|z-z_0|). \tag{16}$$

which satisfies the normality condition $\int_V g(\mathbf{r})d\mathbf{r}=1$. In Eq. (16) z_0 is the coordinate of the center of radiating region, and h, d are the thickness and diameter of this region accordingly.

Let us produce the calculation of spectrum of electromagnetic radiation generated by discharges in the atmosphere region in which electric field reaches the breakdown value. In this case, the occurrence of the spatial irregularities of electric charge leads to local regions of electric field enhancement. Electric discharge arises in such local regions. The occurrence of electric charge irregularities can be related to the atmosphere turbulence and the dissipative instability of charged aerosol stream (Grach et al., 2005). Spatial scale of irregularities l in both cases has the same order of quantity (1–10) m. We estimate the mean-square value of current amplitude I_0 in the charge. Electric field reaches the breakdown value as a result of deviation from the equilibrium value of charge $\pm q$ inside the irregularity with characteristic size l. This field has a value of the order of $E=q/\varepsilon_0 l^2$. The discharge occurs when the electric field reaches the breakdown value $E=E_k$ inside the irregularity. Consequently, the quantity of charge is defined by the size of irregularity$q=\varepsilon_0 l^2 E_k$. The amplitude of current flowing into the discharge for time τ has a quantity $I_0=q/\tau=\varepsilon_0 l^2 E_k/\tau$. Taking into account that the wave of current in the discharge has the velocity $u=1/\tau$ (Bazelyan and Raizer, 2000) one finds

$$I_0=\varepsilon_0 u l E_k.$$

Let us make an estimation of current quantity I_0. Breakdown field at the altitude (5–10) km has the value of the order of $E_k=10^5$ V/m. According to the observation of lightning discharges the velocity of discharge wave has the value of the order of $u=(10^7–10^8)$ m/s (Betz et al., 2009) , and occurrence frequency of discharges has the value $\nu=2\times 10^5\ \mathrm{s}^{-1}$ (Iudin and Trakhtengerts, 2001). Taking into account $l=10\,\mathrm{m}$, $u=10^8\,m/s$, $\tau=10^{-7}\,\mathrm{s}$, one finds $I_0=50$ A. We suggest that discharges formed in the region of atmosphere are described by the parameters $d=40\,\mathrm{km}$, $h=1\,\mathrm{km}$, $z_0=6\,\mathrm{km}$ as depicted in Fig. 3 (lower panel, right graphic).

We compare our results with the data of measurements in Ruzhin and Nomicos (2007). For comparison we have calculated the electric field amplitude of radiation at the frequency of $f=\omega/2\pi=50\,\mathrm{MHz}$ with spectral interval $\Delta f=20$ kHz by the formula

$$E(\mathbf{r},f,\Delta f)=\sqrt{P(\mathbf{r},2\pi f)\Delta f}.$$

According to this formula and Eqs. (14) and (16), the electric field at a distance 300 km from the epicenter has a value $E(\mathbf{r},f,\Delta f)=6.5\times 10^{-6}\,V/m$. The result of estimations is compared with the value of radiation field observed in Ruzhin and Nomicos (2007) at distances (300–350) km from the epicenter of preparing

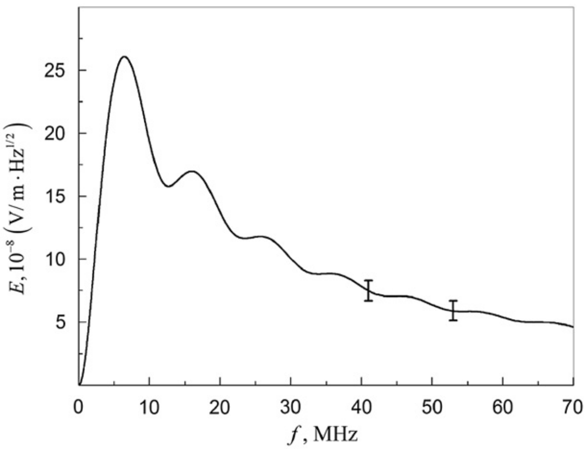

Fig. 5. Spectrum of electromagnetic radiation at distance 300 km from the epicenter. The vertical sections of line denote the experimental data. The following parameters are chosen for calculations: $I_0=50\mathrm{A}$, $\nu=2\times 10^5\,\mathrm{s}^{-1}$, $u=10^8\,m/s$, $\tau=10^{-7}\,\mathrm{s}$, $\alpha=2\times 10^7\,\mathrm{s}^{-1}$, $\beta=8\times 10^7\,\mathrm{s}^{-1}$, $d=40\,\mathrm{km}$, $h=1\,\mathrm{km}$, $z_0=6\,\mathrm{km}$.

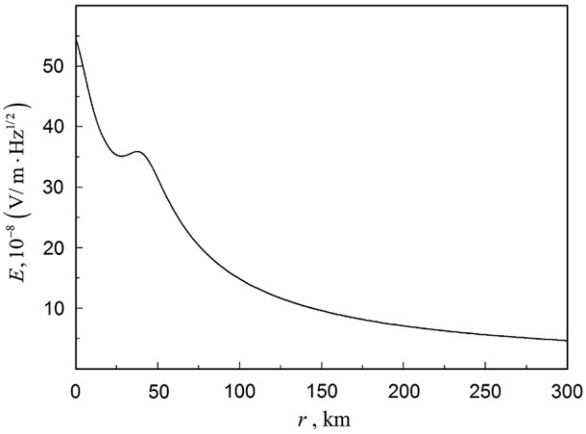

Fig. 6. Dependence on distance of the amplitude of electromagnetic radiation at a frequency 50 MHz. The following parameters are chosen for calculations: $I_0=50\mathrm{A}$, $\nu=2\times 10^5\,\mathrm{s}^{-1}$, $u=10^8\,m/s$, $\tau=10^{-7}\,\mathrm{s}$, $\alpha=2\times 10^7\,\mathrm{s}^{-1}$, $\beta=8\times 10^7\,\mathrm{s}^{-1}$, $d=40\,\mathrm{km}$, $h=1\,\mathrm{km}$, $z_0=6\,\mathrm{km}$.

EQs. Radiation spectrum at distance 300 km calculated by Eqs. (15) and (16) is depicted in Fig. 5. The spectrum has a maximum value at frequency of the order of 10 MHz. The amplitude of radiation in the spectral interval (30–70) MHz is less by three times than its maximal value. Radial dependence of the electric field of radiation at the frequency of 50 MHz is depicted in Fig. 6. The amplitude of field decreases depending on the epicenter distance.

5. Conclusion

Permanent monitoring of the electromagnetic VHF radiation for three-year period in Greece shows that the generation region is located at altitudes (1–10) km in the atmosphere above the epicenter of an EQ area. The radiation is observed during several days before an EQ. Enhancement of the DC electric field up to the value of the order of 10 mV/m in the ionosphere is observed by the satellite during the same period. The occurrence of such a strong DC electric field in the ionosphere is related to the electric current flowing into the atmosphere–ionosphere circuit. The current source is an electromotive force in the ground-air layer occurring by injection of charged aerosols with soil gases in the atmosphere during seismic activity. The electric field of conducting current flowing between the atmosphere and ionosphere can reach the breakdown value in the lower atmosphere. Electric field forms the electric discharges in this region of the atmosphere which are the source of VHF radiation. Calculation results of the amplitude and frequency characteristics of radiation are convincingly confirmed by the observation data. It can be assumed that the enhancement of ionization in the atmosphere region with discharges can lead to the radio wave refraction on the path of their propagation close to the disturbed area.

Appendix

The power spectrum of electromagnetic radiation

$$P(\mathbf{r},\omega)=\lim_{T\to\infty}\frac{|E_T(\mathbf{r},\omega)|^2}{T};\quad E_T(\mathbf{r},\omega)=\int_0^T \exp(i\omega t)E(\mathbf{r},t)\,dt. \tag{A1}$$

is calculated using the temporal dependence of electric field during a long time interval T. The function $E_T(\mathbf{r},\,\omega)$ is defined by an integral in Eq. (A1). The function $E(\mathbf{r}, \omega)$ is calculated by Eq. (8)

$$E(\mathbf{r},\omega) \approx a(\omega)\sum_k j_k G(\mathbf{r}-\mathbf{r}_k,\omega)\sum_m \exp(i\omega t_{km})$$

$$a(\omega) = \int_V A(\mathbf{r}',\omega)\, d\mathbf{r}'.$$

In this formula the summation of terms is performed over time moments $t_{km} < T$. We denote ν as the average frequency of discharges, and the quantity of discharges in the time interval T is $N=\nu T$. Substituting Eq. (8) in (A1), deriving summation and statistical averaging according to Eq. (6)

$$\langle \exp(i\omega t_{km})\rangle = 0; \quad \langle \exp(i\omega t_{km})\exp(-i\omega t_{in})\rangle = \delta_{ki}\delta_{mn}.$$

one finds the formula for the power spectrum of electromagnetic radiation in the form

$$P(\mathbf{r},\omega) = \langle j_k^2 \rangle |a|^2 \frac{\nu}{N}\sum_k |G(\mathbf{r}-\mathbf{r}_k,\omega)|^2 N_k; \quad \sum_k N_k = N. \tag{A2}$$

where N_k is the number of discharges in the cell with radius-vector $\mathbf{r}_k$, N_k/N is the relative number of discharges in the cell with radius-vector $\mathbf{r}_k$, J is the mean-square value of current density of k discharges. Let us assume that the probability of discharge occurrence ΔK in the time interval $(t,\ t+\Delta t)$ does not depend on time $\Delta K=\nu\Delta t$. The relative number of discharges is defined by the formula

$$\frac{N_k}{N} = g(\mathbf{r}_k)\Delta V_k; \quad \sum_k g(\mathbf{r}_k)\Delta V_k = 1. \tag{A3}$$

where ΔV_k is the volume of cell with number k, $g(\mathbf{r}_k)$ is the probability density of discharges distribution on cells with radius-vector $\mathbf{r}_k$. Substituting Eq. (A3) in (A2) and changing summing over k to the integration over the volume V in Eq. (A2), one finds

$$P(\mathbf{r},\omega) = \langle j_k^2 \rangle |a(\omega)|^2 \nu \int_V g(\mathbf{r}')|G(\mathbf{r}-\mathbf{r}',\omega)|^2 d\mathbf{r}'; \quad \int_V g(\mathbf{r})d\mathbf{r} = 1.$$

Taking into account Eq. (4), we obtain from this equation

$$P(\mathbf{r},\omega) = \langle j_k^2 \rangle |a(\omega)|^2 \frac{\mu_0^2 \nu\omega^2}{4\pi^2}\int g(\mathbf{r}')\frac{1}{R^2}\left(1-\frac{z_1^2}{R^2}\right)^2 d\mathbf{r}'.$$

We suggest the horizontal distribution of a radiation source to be axially symmetric. The power spectrum of radiation in the cylindrical coordinates (ρ,φ,z) has the following form:

$$P(\rho,\omega) = \langle j_k^2 \rangle |a(\omega)|^2 \frac{\mu_0^2 \nu\omega^2}{2\pi}\int_0^\infty \rho_1 d\rho_1 \int_0^\infty dz_1 \frac{g(\rho_1,z_1)}{r^2\sqrt{1-p^2}} \times\left[1-\frac{2z_1^2}{r^2}\frac{1}{1-p^2}+\frac{z_1^4}{r^4}\frac{1+p^2/2}{(1-p^2)^2}\right]. \tag{A4}$$

References

Betz, H.D., Schumann, U., Laroche, P., 2009. Lightning: Principles, Instruments and Applications. Springer.

Berger, K., Anderson, R.B., Kroninger, H., 1975. Parameters of lightning flashes. Electra 41, 23–37.

Bazelyan, E.M., Raizer, Y.P., 2000. Lightning Physics and Lightning Protection. CRC Press, pp. 325.

Chmyrev, V.M., Isaev, N.V., Bilichenko, S.V., Stanev, G.A., 1989. Observation by space-borne detectors of electric fields and hydromagnetic waves in the ionosphere over on earthquake centre. Phys. Earth Planet. Inter. 57, 110–114.

Gousheva, M., Danov, D., Hristov, P., Matova, M., 2008. Quasi-static electric fields phenomena in the ionosphere associated with pre- and post earthquake effects. Nat. Hazards Earth Syst. Sci. 8, 101–107.

Grach, V.S., Demekhov, A.G., Trakhtengerts, V.Y., 2005. Kinetic instability of charged particle flow in a thunderstorm cloud. Radiophys. Quantum Electron. 48 (6), 435–446.

Hayakawa, M., Molchanov, O.A. (Eds.), 2002. Seismo Electromagnetics: Lithosphere–Atmosphere–Ionosphere Coupling. TERRAPUB, Tokyo.

Hayakawa, M. (Ed.), 2009. Electromagnetic Phenomena Associated with Earthquakes. Transworld Research Network, Trivandrum (India).

Hayakawa, M., Ohta, K., Maekawa, S., Yamauchi, T., Ida, Y., Gotoh, T., Yonaiguchi, N., Sasaki, H., Nakamura, T., 2006. Electromagnetic precursors to the 2004 Mid Niigata Prefecture earthquake. Phys. Chem. Earth 31, 356–364.

Hata, M., Tian, X., Takumi, I., et al., 1996. ELF horizontal flux precursor of moderate M5.8 Yamanashi 96 inland earthquake—a general approach to electromagnetic wave precursor. J. Atmos. Electr. 16 (3), 199–220.

Hata, M., Takumi, I., Yabashi, S., 1998. A model of earthquake seen by electromagnetic observation—gaseous emission from the Earth as main source of pre-seismic electromagnetic precursor and trigger of followed earthquake. Ann. Geophys. 16, C1188–C1197.

Iudin, D.I., Trakhtengerts, V.Y., 2001. Fractal structure of the nonlinear dynamics of electric charge in a thundercloud. Radiophys. Quantum Electron. 44 (5–6), 386–402.

Maeda, K., Tokimasa, N., 1996. Decametric radiation at the time of the Hyogo-ken Nanbu earthquake near Kobe in 1995. Geophys. Res. Lett. 23 (18), 2433–2436.

Molchanov, O.A., Hayakawa, M., 2008. Seismo Electromagnetics and Related Phenomena: History and Latest Results. TERRAPUB, Tokyo 189p.

Nomicos, C., Vallianatos, F., Kalliakatos, J., Sideris, F., Bakatsakis, M., 1995. Latest aspects of telluric and electrmagnetic variations associated with shallow and intermediate depth earthquakes in South Aegean. Ann. di Geophys. X1/2, 361–375.

Proctor, D.I., 1981. VHF radio pictures of cloud flashes. J. Geophys. Res. 86 (C5), 4041–4071.

Ruzhin, Yu.Ya., Nomicos, C., Vallianatos, F., 1999. VHF precursor generated in atmosphere before earthquake, report SE27-017. In: Proceedings of 24th General Assembly of EGS, Haague, Geophysical Research 105.

Ruzhin, Yu.Ya., Nomicos, C., Vallianatos, F., 2000. High frequency seismoprecursor emissions. In: Proceedings of 15th Wroclaw EMC Symposium, pp. 512–517.

Ruzhin, Yu., Nomicos, C., 2007. Radio VHF precursors of earthquakes. Nat. Hazards 40, 573–583.

Rytov, S.M., Kravtsov, Yu.A., Tatarsky, V.I., 1978. Principles of Statistical Radiophysics—Pt. 1. Springer-Verlag, Berlin 345p.

Sorokin, V.M., Chmyrev, V.M., Yaschenko, A.K., 2001. Electrodynamic model of the lower atmosphere and the ionosphere coupling. J. Atmos. Sol.–Terr. Phys. 63 (16), 1681–1691.

Sorokin, V.M., Chmyrev, V.M., 2002. Electrodynamic model of ionospheric precursors of earthquakes and certain types of disasters. Geomagn. Aeron. 42, 784–792.

Sorokin, V.M., Chmyrev, V.M., Yaschenko, A.K., 2005. Theoretical model of DC electric field formation in the ionosphere stimulated by seismic activity. J. Atmos. Sol.–Terr. Phys. 67, 1259–1268.

Sorokin, V.M., Yaschenko, A.K., Chmyrev, V.M., Hayakawa, M., 2006. DC electric field formation in the mid-latitude ionosphere over typhoon and earthquake regions. Phys. Chem. Earth 31, 454–461.

Sorokin, V.M., Yaschenko, A.K., Hayakawa, M., 2007. A perturbation of DC electric field caused by light ion adhesion to aerosols during the growth in seismic-related atmospheric radioactivity. Nat. Hazards Earth Syst. Sci. 7, 155–163.

Sorokin, V.M., Chmyrev, V.M., 2010. Atmosphere–ionosphere electrodynamic coupling. In: Bychkov, V.L., Golubkov, G.V., Nikitin, A.I. (Eds.), The Atmosphere and Ionosphere: Dynamics, Processes and Monitoring. Springer, pp. 97–146 isbn:978-90-481-3211-9.

Taylor, W.L., 1978. A VHF technique for space-time mapping of lightning discharge processes. J. Geophys. Res. 83 (C7), 3575–3583.

Vallianatos, F., Nomicos, K., 1998. Sesmogenic radioemissions as earthquake precursors in Greece. Phys. Chem. Earth 23 (9–10), 953–957.

Voinov, V.V., Gufeld, I.L., Kruglikov, V.V., et al., 1992. Effects in the ionosphere and atmosphere before the Spitack earthquake, News of USSR Academy. Fiz. Zemli (3), 96–101 (in Russian).

Warwick, J.W., Hayenga, C.O., Brosnahan, J.W., 1979. Interferometric directions of lightning sources at 34 MHz. J. Geophys. Res. 84 (C5), 2457–2467.

Warwick, J.W., Stoker, C., Maer, T.R., 1982. Radioemission associated with rock fracture: possible application to the great Chillean earthquake of May 22, 1960. J. Geophys. Res. 87, 2851–2859.

Williams, E.R., 1989. The electrification of thunderstorms. J. Geophys. Res. 93 (D6), 992–993.

Yamada, A., Sakai, K., Yaji, Y., Takano, T., Shimakura, S., 2002. Observation of natural noise in VHF band which relates to earthquakes. In: Hayakawa, M., Molchanov, O.A. (Eds.), Seismo Electromagnetics: Lithosphere–Atmosphere–Ionosphere Coupling. TERRAPUB, Tokyo, pp. 255–257.

Yonaiguchi, N., Ida, Y., Hayakawa, M., Masuda, S., 2007. A comparison of different fractal analyses for VHF electromagnetic emissions and their self-organization for the off-sea Miyagi-prefecture earthquake. Nat. Hazards Earth Syst. Sci. 7, 485–493.

Yasuda, Y., Ida, Y., Goto, T., Hayakawa, M., 2009. Interferometric direction finding of over-horizon VHF transmitter signals and natural VHF radio emissions possibly associated with earthquakes. Radio Sci. 44, RS2009. doi:10.1029/2008RS003884.

Zhao, Y., Qian, F., 1997. Earthquake lights: a very convincing evidence for energy transfer from earth to air. In: Proceedings of International Workshop on Seismo-Electromagnetics (Abstracts), NASDA, Tokyo 242.